Research Article

Received: 4 February 2018 Revised: 16 February 2018 Accepted article published: 25 March 2018 Published online in Wiley Online Library: 13 May 2018

(wileyonlinelibrary.com) DOI 10.1002/pi.5586

Effect of annealing time and molecular weight on melt memory of random ethylene 1-butene copolymers

Xuejian Chen, Chen Qu and Rufina G Alamo*

Abstract

The effects of annealing time and molecular weight on the strong melt memory effect observed in random ethylene 1-alkene copolymers are analyzed in a series of model ethylene 1-butene copolymers with 2.2 mol% branches. Melt memory is associated with molten clusters of ethylene sequences from the initial crystals that remain in close proximity and are unable to diffuse quickly to the randomized melt state, thus increasing the recrystallization rate. Melt memory persists even for greater than 1000 min annealing indicating a long-lived nature of the clusters that only fully dissolve at melt temperatures above a critical value (>160 °C). Below the critical melt temperature, molecular weight and annealing temperature have a strong influence on the slow kinetics of melt memory. For the copolymers analyzed, slow dissolution of clusters is experimentally observed only for $M_w < 50\,000$ g mol^{-1}. More stable clusters that survive higher annealing temperatures display slower dissolution rates than clusters remaining at lower temperatures. The threshold crystallinity level to enable melt memory ($X_{c,threshold}$) decreases with increasing molecular weight and decreasing annealing temperature similarly to the variation of the chain diffusivity in the melt. The process leading to melt memory is thermally activated as the variation of $X_{c,threshold}$ with temperature follows Arrhenius behavior with high activation energy (*ca* 108 kJ mol^{-1}) that is independent of molecular weight.

Keywords: melt memory; crystallization; ethylene copolymers; melt annealing

INTRODUCTION

Avenues to control the rate of polymer crystallization have long been of industrial interest. Faster solidification enhances the stability of the material processed and shortens the production cycle, leading to economically favored processes. It is well known that polymer crystallization from the disordered melt state involves two stages, nucleation and crystal growth, of which the nucleation step drives the overall crystallization rate. Hence, often in industrial settings, external nucleating agents are added to decrease the nucleation barrier in order to accelerate crystallization. It has also been demonstrated that self-nucleation can be highly effective in increasing crystallization rate.[1,2] The number of nuclei induced by self-nucleation can overcome, by several orders of magnitude, the number of commonly found heterogeneous nuclei in a bulk polymer. If melting is incomplete, traces of crystallites act as seeds to bypass the primary nucleation barrier upon recrystallization.[1,3] Other sources of self-nucleation can be found in melts at temperatures a few degrees above the observed melting point. For example, it has been posited that self-nuclei may derive from residual orientation of chain segments that formed the initial crystallites,[4–6] from residual intermolecular interactions,[7–9] from a heterogeneous distribution of crystalline sequences[10–14] or from inhomogeneous entanglement redistribution.[15,16]

In homopolymers, the memory effect is mostly observed below the equilibrium melting temperature and near the observed melting resulting in higher crystallization temperatures or higher rates of crystallization, smaller spherulites and even modifications of the crystal lattice in systems that display polymorphism.[1,17–24] Below the equilibrium melting temperature, the polymer melt is undercooled and the possibility of crystallites surviving in the melt cannot be excluded. Often for homopolymers, melt memory disappears after increasing holding time in the melt and the kinetics become reproducible.[5,22,25] Supaphol *et al.*[19] studied the recrystallization of syndiotactic polypropylene (s-PP) from 150 °C (*ca* 30 °C below the equilibrium melting temperature of s-PP[26]) and found that it took *ca* 250 min to erase self-nuclei. Similarly, it took about 120 min to erase memory at 168 °C in the melt of isotactic polypropylene (iPP).[6] In linear polyethylene, a critical holding time of up to 80 min may be required at temperatures above the equilibrium melting point for complete melt randomization depending on the molecular weight.[25]

In recent works it has been found that random copolymers of ethylene display memory of crystallization even at temperatures *ca* 30 degrees above their equilibrium melting points. This unusually strong melt memory of copolymers is in sharp contrast with the behavior of linear polyethylene fractions that, independent of molar mass, display memory at temperatures well below the equilibrium melting temperature.[10] A copolymer's strong memory is associated with the process of sequence partitioning during

* *Correspondence to: RG Alamo, Department of Chemical and Biomedical Engineering, FAMU-FSU College of Engineering, 2525 Pottsdamer St, Tallahassee, FL 32310-6046, USA. E-mail: alamo@eng.fsu.edu*

Department of Chemical and Biomedical Engineering, FAMU-FSU College of Engineering, Tallahassee, FL, USA

Table 1. Molecular characterization of HPBDs with *ca* 2.2 mol% ethyl branches

Sample	Branch type	Branch content (mol%)	M_w (g mol^{-1})	PDI	$T_m^\circ{}_{copo}$ (°C)[a]
P16	Ethyl	2.1	16 000	1.4	138.0
P24	Ethyl	2.3	24 000	1.1	137.3
P49	Ethyl	2.22	49 000	1.1	137.6
P108	Ethyl	2.2	108 000	1.1	137.7
P120	Ethyl	2.2	120 000	1.1	137.7
P195	Ethyl	1.95	214 500	1.1	138.6
P420	Ethyl	2.22	420 000	1.84	137.6

[a] Calculated with Flory's equation[34] using T_m° (homopolymer) =145.5 °C, and $\Delta H^0 = 290$ J g^{-1}.

crystallization. Because branches longer than methyl are excluded from the crystal, the crystallization of random copolymers evolves through a process of sequence length selection by which long ethylene sequences are selected first, and other shorter sequences of suitable length will need to diffuse through the entangled melt to the crystal front in order to propagate lamellar crystallites. The path of selecting and dragging ethylene sequences to build copolymer crystallites generates a complex topology of branches, knots, loops, ties and other entanglements in the intercrystalline regions, especially at high levels of transformation, which is viewed as being responsible for the unusually strong melt memory observed in random ethylene copolymers.[10,27]

It is reasonable to assume that when the crystallites of ethylene copolymers melt, clusters from the initial crystalline ethylene sequences remain in close proximity, because segmental melt diffusion to randomize all sequences is hampered by branches and the constrained intercrystalline topology. Although these remains of sequence partitioning can be taken as a weak phase separation in the melt,[28,27] melts with this type of memory are metastable systems where the clusters are effective pre-nuclei that only fully dissolve into a homogeneous melt at temperatures well above the equilibrium melting point.[10,11] Segmented thermoplastic polyurethanes are also examples of systems with sequence selective crystallization, and have also shown relatively strong melt memory.[14]

The experimental evidence is consistent with a kinetic nature of melt memory.[5,6,10,11,15,23,29–32] Even when cooling from the same melting temperature, the increase of crystallization temperature depends on molecular weight, the initial level of crystallinity or on how the standard crystalline state is prepared. However, systematic studies of the effect of melt annealing on residual melt memory are scarce. Of relevance are recent works on the long-lived nature of melt flow-induced precursors of crystallization of iPP and propylene ethylene random copolymers.[30,32] Compared with thermal nuclei from quiescent melts, flow-induced precursors required higher temperatures and longer time to dissolve and thus contribute to memory effects above the equilibrium melting temperature of iPP (208 °C). Complete elimination of the flow-induced memory effect required *ca* 3000 min of annealing (more than 2 days) at a temperature just above equilibrium (210 °C). Even at 250 °C, *ca* 300 min of annealing is required for erasing persistent memory of the flow-induced precursors. Hashimoto *et al.*[33] also demonstrated by time-dependent experiments with isotactic polystyrene (iPS) that spherulite nuclei formed by quenching and subsequent annealing are more stable and persist longer in the melt compared to those formed just by quenching or only by annealing.

Very slow kinetics were also inferred for dissolution of the observed strong melt memory of random ethylene copolymers.[10,11] Annealing the melt of a copolymer with $M_w = 108\,000$ g mol^{-1} at 150 °C for up to 3 h rendered no significant changes upon recrystallization. Hence, it appears that dissolution of the clusters is also a very slow process even at temperatures 40–50 degrees above the observed melting. However, the effect of melt annealing on memory was not tested for lower molecular weights with inherent enhanced melt diffusion. We address the dependence of copolymer molecular weight and melt temperature on melt memory in the present work and we also extend the annealing times to >1000 min. Additionally, the dependence of the threshold level of crystallinity on molecular weight and melt temperature is also quantified. The characteristic times related to dissolution of melt memory and the threshold crystallinity level that enables the manifestation of melt memory follow the behavior of thermally activated processes for which the activation energies are estimated.

EXPERIMENTAL

Materials

A series of hydrogenated polybutadienes (HPBDs), which are analogous to random ethylene 1-butene copolymers, are used in this study. These HPBDs feature similar branching content (*ca* 2.2 mol%), molecular weights ranging from 16 000 to 420 000 g mol^{-1} and very narrow polydispersity index (PDI). The molecular characterization is summarized in Table 1. All the samples, including P195 not studied in our previous work,[10] show melt memory above the equilibrium melting temperature ($T_m^\circ{}_{copo}$).

Besides the original HPBDs, a 25/75 binary blend of P16/P49 was prepared by co-precipitation from dilute solution. The two HPBDs, P16 and P49, with mass ratio of 25:75 were dissolved in hot xylene at *ca* 120 °C and subsequently precipitated in chilled acetone. After filtration, the blend was dried inside a fume hood overnight and further in a heated oven (*ca* 70 °C) under vacuum for *ca* 4 h.

Melt annealing time dependence experimental protocol

Samples were prepared as films (*ca* 30 μm thick) by melt-pressing between Teflon sheets in a Carver press at *ca* 150 °C and subsequent quenching between two steel plates. A single piece weighing *ca* 4 mg was cut from the center of the film and encapsulated in an aluminium pan. Crystallization and melting were followed using a TA Q2000 differential scanning calorimeter connected with an intercooler. The instrument was operated under nitrogen environment. Calibrations for static temperature, thermal lags and heat of fusion were performed with indium. Melt annealing

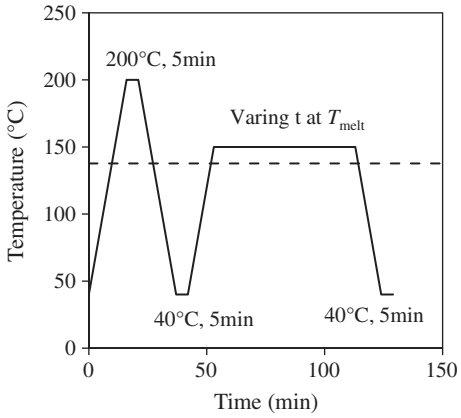

Figure 1. Thermal protocol of melt annealing time-dependent experiments followed using DSC. The horizontal dashed line represents the equilibrium melting temperature $T_m^\circ{}_{copo}$.

time-dependent experiments were carried out with the thermal protocol sketched in Fig. 1. The sample was first melted at 200 °C to erase thermal history and subsequently cooled to 40 °C to prepare a standard crystalline state, followed by heating to a fixed heterogeneous melt temperature (T_{melt}) above $T_m^\circ{}_{copo}$ and subsequently cooling back to 40 °C. All heating and cooling ramps were at 10 °C min^{-1}. Except for changing annealing times at heterogeneous T_{melt}, 5 min holding time was given at each target temperature in order to ensure temperature stabilization. The thermal protocol was repeated while increasing the holding time (t), up to 1200 min, at the heterogeneous T_{melt} in successive cycles. The crystallization peak temperature ($T_{c,peak}$) from both the melt at 200 °C and the selected heterogeneous T_{melt} were recorded in each cycle and the difference $\Delta T_{c,peak}$ was evaluated as a function of holding time.

The time-dependent annealing experiments were performed on four HPBDs with molecular weights changing from 16 000 to 108 000 g mol^{-1} (P16, P24, P49, P108) and for the 25/75 blend of P16/P49 at the same heterogeneous T_{melt} (140 °C). The range of heterogeneous T_{melt} was determined based on typical T_{melt} *versus* $T_{c,peak}$ plots for each sample.[10] Representative cooling from different T_{melt} and heating thermograms are shown in Fig. 2(a) for P16 as an example. The temperature at the peak of the exotherm, $T_{c,peak}$ (magnified in the inset of Fig. 2(a)), was recorded as a function of the initial T_{melt}. These data are plotted in Fig. 2(b). Strong melt memory is observed as an increase of $T_{c,peak}$ with lowering T_{melt} in a range from 160 °C ($T_m^\circ{}_{copo}$) to 138 °C ($T_{critical}$, the critical T_{melt} to erase memory effect). The range of heterogeneous T_{melt} is accordingly determined. To investigate the effect of temperature on dissolution of melt memory, time-dependent experiments were followed at various heterogeneous T_{melt} in P16.

Crystallinity effect experimental protocol

The DSC thermal protocol depicted in Fig. 3 was used to assess the effect of the initial level of crystallinity on melt memory and to determine the minimum amount of crystallinity ($X_{c,threshold}$) required for observing the strong memory effect on crystallization. The sample was initially heated to 200 °C to establish a homogeneous melt and subsequently cooled to a certain temperature T_1 for partial crystallization and held for 5 s which is approximately the response time of DSC to actually reach the set temperature. After 5 s at T_1, the temperature was raised to a heterogeneous T_{melt}, kept at this temperature for 5 min and cooled to record the crystallization peak ($T_{c,peak}$) as a function of the initial level of crystallinity. The initial level of crystallinity was calculated from the endotherm of the heating run from T_1 to T_{melt}. The holding time at any temperature other than T_1 was 5 min. The thermal protocol was repeated with lowering T_1 in successive cycles to achieve higher crystallinity levels prior to approaching heterogeneous T_{melt}. Various T_1 were chosen within the span of the crystallization exotherm from the homogeneous melt as detailed in a prior work.[29]

Crystallinity-dependent experiments were conducted for all HPBDs listed in Table 1 at the same heterogeneous T_{melt} (140 °C) to investigate the molecular weight dependence of $X_{c,threshold}$. Additional experiments were conducted with different heterogeneous T_{melt} on P108 and P195 in order to address the effect of melt temperature on $X_{c,threshold}$.

RESULTS AND DISCUSSION

Effect of melt annealing time on melt memory

Molecular weight dependence of annealing process

The effect of annealing time at a fixed heterogeneous T_{melt} (140 °C) was first analyzed in HPBDs with molecular weights in a range from 16 000 to 108 000 g mol^{-1} (P16, P24, P49 and P108). Figure 4(a) displays representative examples of crystallization exotherms of P16 during cooling from a melt of 200 °C (homogeneous) and from a melt of 140 °C (heterogeneous) after various melt annealing times. The exotherms from 200 °C are independent of annealing time, but the exotherms from 140 °C shift to lower temperatures with increasing annealing time as indicated by the arrows in the figure. Notice that a cooling run from 200 °C (held for 5 min) was always recorded after cooling from 140 °C and prior to the subsequent run with increasing annealing time. Such runs from 200 °C are used as a reference point to eliminate any possible drift in the homogeneous melt. As seen by the open symbols in Fig. 4(b), the HPBDs are very stable since drifts in $T_{c,peak}$ from 200 °C during the annealing experiments are insignificant. The decrease of $T_{c,peak}$ as a function of annealing time at 140 °C is given by the filled symbols in Fig. 4(b). Even after 1200 min annealing at 140 °C the absolute decrease in $T_{c,peak}$ that is associated with dissolution of memory is relatively small, less than one degree; however, it corresponds to a *ca* 35% in reduction of memory in reference to the $T_{c,peak}$ value from a melt free of memory. These data indicate that although of a kinetic nature, the clusters associated with melt memory are remarkably stable since even for this relatively low molecular weight it will take an unduly long time to dissipate them to levels close to the melt free of memory.

The difference between $T_{c,peak}$ cooling from 200 °C and the value from 140 °C represents the extent of melt memory ($\Delta T_{c,peak}$), or content of memory left in a heterogeneous melt. The variation of $\Delta T_{c,peak}$ with annealing time is shown in Fig. 5(a) for P16 and in Fig. 5(b) for the rest of the copolymers investigated. The data for P16 show an exponential decay with time spent at 140 °C, similar to the exponential decay observed for dissolution of memory in iPP.[6] For a more direct comparison, the $\Delta T_{c,peak}$ values of copolymers shown in Fig. 5(b) are shifted vertically to match the first point of P16 at 5 min. It is in such way that the change in $T_{c,peak}$ at a given annealing time with molecular weight is emphasized. It is clear that the kinetics of dissolution of memory are a strong decreasing function of molecular weight. We recall from our prior studies that HPBDs with M_w less than *ca* 10 000 g mol^{-1} do not have strong melt memory.[10] The present data indicate that as the copolymer develops stronger melt memory with increasing molar mass, the

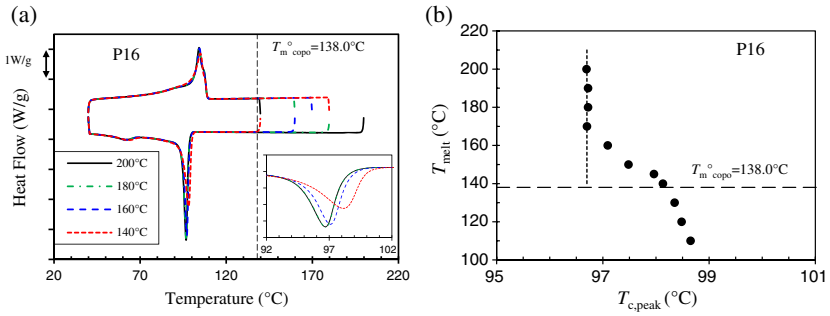

Figure 2. (a) Plot of heat flow against temperature for cooling from various T_{melt} (indicated in the legend) and subsequent heating at 10 °C min^{-1} for P16. The black vertical dashed line represents the equilibrium melting temperature of this copolymer ($T_m^{\circ}{}_{copo}$). Differences in crystallization exotherms are magnified in the inset. (b) Plot of the initial T_{melt} *versus* the subsequent $T_{c,peak}$ for P16. The horizontal dashed line represents $T_m^{\circ}{}_{copo}$.

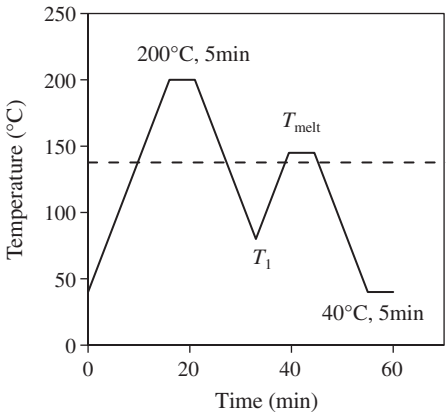

Figure 3. Schematic cycling temperature diagram to study the effect of level of crystallinity, achieved by dynamic cooling at 10 °C min^{-1}, on melt memory. The level of crystallinity is changed by changing T_1. The horizontal dashed line represents $T_m^{\circ}{}_{copo}$.

memory is more difficult to dissolve. As seen in Fig. 5(b), P16 shows a 0.8 °C decrease in $\Delta T_{c,peak}$, while P24, with M_w of 24 000 g mol^{-1}, exhibits only a 0.4 °C reduction in $\Delta T_{c,peak}$ over 20 h in the melt. P49 (M_w = 49 000 g mol^{-1}) displays an even smaller decrease (<0.1 °C) with almost constant $\Delta T_{c,peak}$ over time. P108 with the highest molecular weight (M_w = 108 000 g mol^{-1}) among the four HPBDs examined displays some drift of $\Delta T_{c,peak}$ towards higher values for low annealing times and a constant $\Delta T_{c,peak}$ at longer annealing times. Data for HPBDs with higher molar masses do not show any change with annealing time. It is feasible that such slow or lack of dissolution of memory is associated with the increase of viscosity in the melt and the corresponding increase of entanglements and topological restrictions to randomize the ethylene sequences of the initial crystals as the molecular weight increases.[35] This assertion is further corroborated by the melt annealing behavior of a 25/75 blend of P16/P49. While P49 displays an insignificant change of melt memory with annealing time at 140 °C, the blend clearly shows the dissolution effect indicated by the open-symbols of Fig. 5(b). The low-molar-mass chains aid segmental diffusion and the dissolution of clusters. A similar molecular weight effect on melt memory is inferred from data of propylene ethylene copolymers and a poly(L-lactic acid) stereocomplex.[36,37]

Melt temperature dependence of annealing process

The effect of melt temperature on the dissipation of melt memory was addressed in P16, the HPBD that shows the largest change in $\Delta T_{c,peak}$, by time-dependent experiments performed at different heterogeneous T_{melt} in a range of 140–151 °C. The variation of $\Delta T_{c,peak}$ with annealing time for all the heterogeneous T_{melt} studied is given in Fig. 6. As expected, the initial extent of melt memory decreases with increasing T_{melt}, but even after 1200 min at the highest T_{melt}, the data are far from zero or far from the state where all memory is dissolved. All data appear to reach an asymptotic value that decreases with T_{melt}.

The continuous lines in Fig. 6 fit the data with the exponential relation proposed by Ziabicki and Alfonso[17,38] for describing the melt time dependence of crystalline memory:

$$\Delta T_{c,peak} = ae^{-t/\tau} + b \quad (1)$$

Here, a is the pre-exponential index representing the total change of $\Delta T_{c,peak}$ over infinite holding time, τ is the characteristic time associated with the dissolution of memory and b is a constant term representing the asymptotic $\Delta T_{c,peak}$ at infinite holding time, which represents some type of stable clusters or long-lived remnants of melt memory. The parameters from the best fits are plotted *versus* annealing temperature in Fig. 7. With increasing T_{melt} both the total change of $\Delta T_{c,peak}$ (a) and the remnant of melt memory (b) decrease, which suggests that not only less memory remains at higher temperature but also the amount of memory that dissolves upon annealing is smaller. In other words, with increasing T_{melt}, the extent of memory left decreases but the clusters that remain, those from the longest sequences, are more stable. The latter is also indicated by the increasing characteristic time (τ) from about 200 to 1000 min with T_{melt}. Such a tendency runs against initial expectations from the variation of diffusivity with temperature and also differs from the observations of Alfonso and coworkers of a faster decay of $T_{c,peak}$ with increasing T_{melt} for iPP.[17] However, Hashimoto *et al.* have recently reported an increase of characteristic times for iPS, related to the decrease of nuclei density upon melt annealing, with increasing melt temperature.[33]

The very long characteristic times associated with dissolution of melt memory observed for HPBDs contrast with relaxation times extracted from various avenues for the same systems. For example, prior work on melt diffusivity for HPBDs at temperatures between 140 and 180 °C with molecular weight ranging from 10 000 to 500 000 g mol^{-1} estimated single chain relaxation times between 1 ms and 10 s.[39–42] These values are 3–7 orders smaller than the characteristic time for dissolution of memory. Hence, dissolution of melt memory appears to entail more than just reptation of polymer chains, because the process of diffusing and randomizing ethylene segments from the initial crystallites is a lot costlier

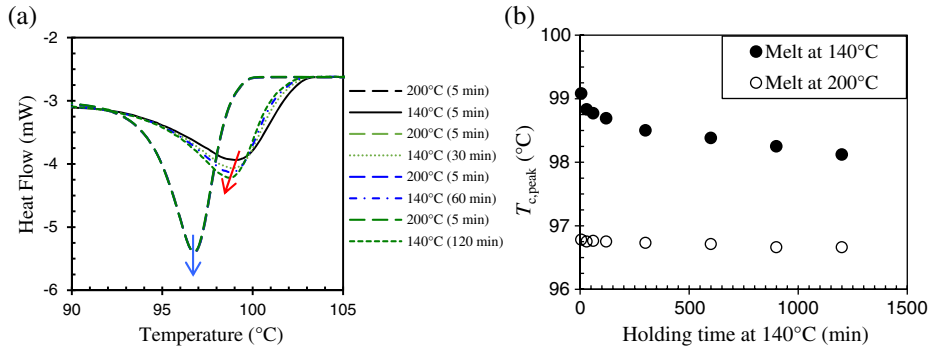

Figure 4. (a) Crystallization exotherms for P16 from a homogeneous T_{melt} (200 °C) and a heterogeneous T_{melt} (140 °C) as a function of annealing time at 140 °C. (b) $T_{c,peak}$ from 200 °C (5 min) and from 140 °C against annealing time at 140 °C.

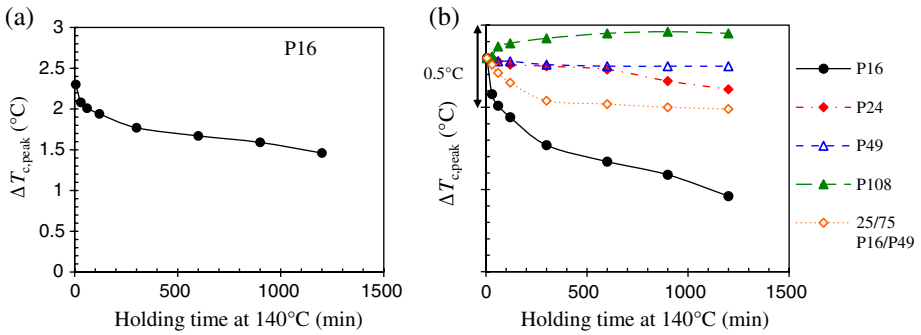

Figure 5. (a) $\Delta T_{c,peak}$ against holding time at 140 °C for P16. (b) $\Delta T_{c,peak}$ (vertically shifted) against holding time at 140 °C for hydrogenated polybutadienes with molecular weight from 16 000 to 108 000 g mol^{-1} and the 25/75 blend of P16/P49.

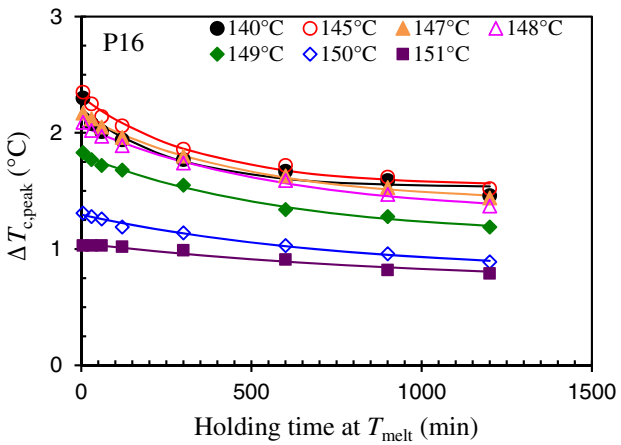

Figure 6. Time dependence of $\Delta T_{c,peak}$ for copolymer P16 for the heterogeneous T_{melt} shown.

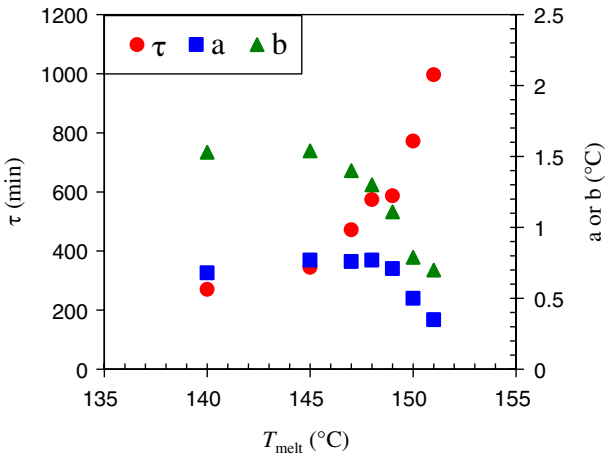

Figure 7. Fitting parameters used in the exponential fit to the $\Delta T_{c,peak}$ time dependence data as a function of T_{melt} for P16.

than the classical translational chain diffusion. Such a discrepancy points to a dissolution process of memory that is uncorrelated with the single-chain dynamics.

For the random copolymers studied here, it is expected that only the longest sequences from the initial crystallites remain clustered at the highest heterogeneous T_{melt}. The long characteristic times increasing with T_{melt}, or small changes observed with time, could be explained considering different metastable states at each heterogeneous T_{melt}, for example as perceived by Muthukumar.[31] This unusual slow kinetics has also been explained considering the system as a weakly phase segregated medium where both sequence segregation and diffusion play a role in the dynamics of cluster dissolution.[12] In this case, upon phase equilibration, sequence re-homogenization may only occur at temperatures above the phase transition. Although a sequence-based phase segregation may explain the unusual stability of melt memory, it does not explain why high levels of crystallinity are needed to observe melt memory, >20% for P16, as shown in the next section. Since it is at the beginning of the crystallization when the longest sequences are selected to be in the crystals, even low levels of crystallinity should lead to a segregated melt, and to melt memory upon heating; but as has been shown,[29] this is not the case, and it is the reason why branches and topological

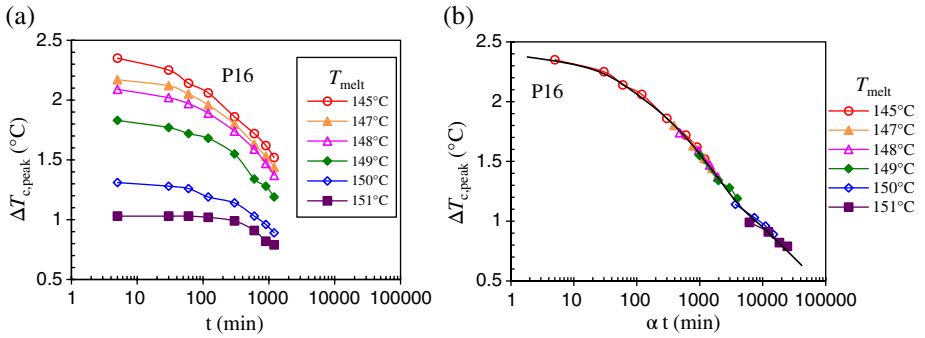

Figure 8. (a) Time (logarithm scale) dependence of $\Delta T_{c,peak}$ from various heterogeneous T_{melt} for P16. (b) Master curve at 145 °C (black solid line) obtained by a horizontal shift of the curves in (a) in reference to the data for $T_{melt} = 145$ °C.

constraints are believed to play a major role in the slow dynamics of copolymer melt memory.

After examination of Fig. 6 in more detail, we notice that the evolution of $\Delta T_{c,peak}$ with annealing time for T_{melt} of 140 and 145 °C is almost identical in spite of a difference of 5 °C in temperature. $\Delta T_{c,peak}$ starts almost at the same value at times close to zero and levels off at the same point for both T_{melt}. Hence, the dependence of cluster dissolution on the initial amount of memory is almost unchanged between T_{melt} of 140 and 145 °C. This occurs because for P16 at T_{melt} below 145 °C the melt is saturated with clusters (notice the small change of $T_{c,peak}$ with decreasing T_{melt} below 145 °C in Fig. 2(b)). A time–temperature superposition analysis is then applied to the data obtained at $T_{melt} \geq 145$ °C. $\Delta T_{c,peak}$ plotted against log of holding time at a fixed T_{melt} is shown in Fig. 8(a). The similarity in curve shape suggests construction of a master curve by fixing the data for T_{melt} of 145 °C and shifting the data for higher T_{melt} horizontally (for annealing times greater than 50 min). The tail part (the last four points) at each T_{melt} falls on the master curve shown by the black solid line in Fig. 8(b).

The shift factors α applied for the time–temperature superposition analysis obey Arrhenius temperature dependence. As shown in Fig. 9, a linear correlation was obtained between ln α and $1000/T_{melt}$, and the slope yields an activation energy of *ca* 1100 kJ mol^{-1}. Such high activation energy is expected from the slow kinetics observed and is about 10 times the value obtained by Milner *et al.*[30] for the dissolution of flow-induced precursors of iPP using the same experimental protocol. The difference may be explained by the comparatively weaker melt memory observed for iPP and iPP–ethylene random copolymers than for polyethylene-based copolymers.[7] This difference has been attributed to a lower melt viscosity of iPP due to a reduced number of entanglements per chain compared to polyethylene.[43,44] Conversely, recent data by Fernandez-Ballester on propylene ethylene random copolymers using a different protocol,[32] and a study by Peters *et al.*[45] on dissolution of flow induced shish structures in high-density polyethylene led to an activation energy of 1200 kJ mol^{-1}, which is very similar to the value for dissipating melt memory of HPBDs studied here.

The difference between the activation energy for dissolution of flow-induced precursors for the crystallization of iPP (120–1200 kJ mol^{-1}) and the activation energy for iPP melt flow (*ca* 40 kJ mol^{-1})[30,32] has been explained as representing activation energies of two steps in the dissolution process. The first and limiting step is the detachment of segments of the oriented bundle which presumably is energetically more costly than the diffusion and randomization of the detached segments into the melt. We could also envision a limiting step to separate the sequences responsible for the copolymer melt memory even if at these high temperatures all crystalline order is lost. The step must be associated with overcoming branches and topological constraints around the clusters because the strong memory effect is not observed in linear polyethylene.[10]

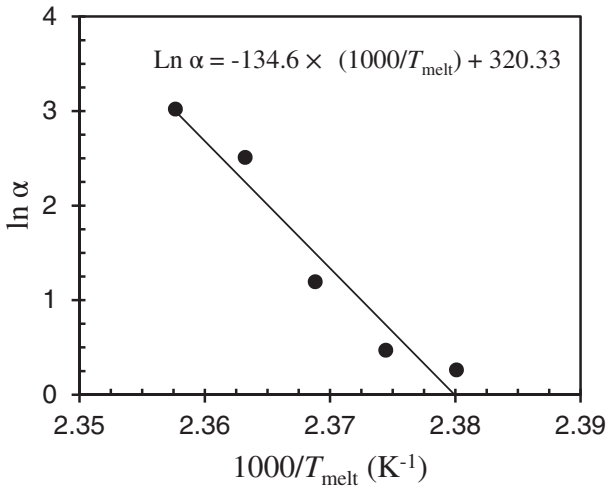

Figure 9. Arrhenius-type temperature dependence of the shift factor α used in the time–temperature superposition analysis in Fig. 8(b) for P16.

Effect of level of crystallinity on melt memory

Molecular weight dependence of threshold level of crystallinity for melt memory

In this section we examine the effect of molecular weight on the threshold crystallinity level ($X_{c,threshold}$) required to observe the initial manifestation of melt memory as an increase in the recrystallization rate. $X_{c,threshold}$ represents the amount of crystals required for building sufficient constraints to prevent dissolution of clusters at a given T_{melt}. The systematics for this study follows the protocols of a prior work.[29] The initial state with different levels of crystallinity was prepared by halting a dynamic cooling from 200 °C at different temperatures T_1 within the exotherm. The crystals were then heated to T_{melt} (5 min) and subsequently cooled to record $T_{c,peak}$. Representative melting endotherms of P16 heating from different T_1 are shown in Fig. 10(a) as examples of increasing crystallinity levels with lowering T_1 from 100 to 40 °C. The degree of crystallinity is calculated from the area of the endotherms using the heat of fusion of the pure crystal as 290 J g^{-1}.[46,47] Subsequent

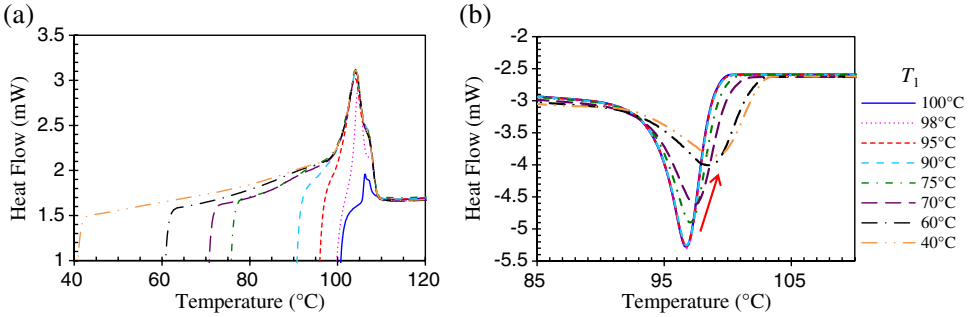

Figure 10. (a) Melting endotherms followed partial crystallization from 200 °C halted at different T_1 for P16. (b) Crystallization from the heterogeneous T_{melt} (140 °C) reached by heating from T_1.

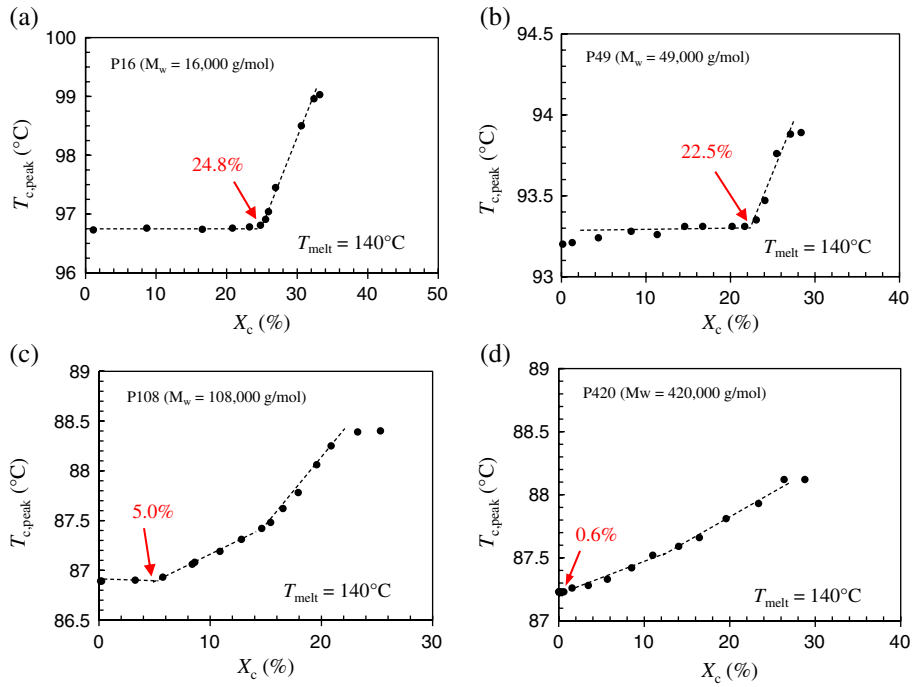

Figure 11. Plots of $T_{c,peak}$ obtained by cooling from 140 °C against initial level of crystallinity (X_c) achieved by non-isothermal crystallization prior to approaching 140 °C. All copolymers have 2.2 mol% ethyl branches. The molecular weight of the HPBD is shown.

crystallization exotherms from a heterogeneous melt temperature of 140 °C are shown in Fig. 10(b). Partial crystallizations halted at T_1 within 100 to 90 °C generate small degrees of crystallinity (<20% for P16) and thus lead to identical crystallization peaks from melt at 140 °C (overlapping with each other). Lowering T_1 from 75 to 40 °C, the initial degree of crystallinity is higher (above the threshold value) and melt memory becomes evident as an increase of the crystallization temperature indicated by the arrow in Fig. 10(b).

The variation of $T_{c,peak}$ with degree of crystallinity for four of the HPBDs analyzed with increasing molecular weight is given in Fig. 11. As shown, up to a molecular weight of about 50 000 g mol^{-1}, the threshold crystallinity level for melt memory at 140 °C is relatively high (>20%) indicating that a high content of crystallites needs to develop from the homogeneous melt in order to retain memory of the crystalline sequence assembly upon subsequent melting. In other words, in this low range of molar mass, all sequences randomize at $T_{melt} \geq 140$ °C if the initial state has less than *ca* 23% crystallinity. The threshold crystallinity level for melt memory decreases sharply for $M_w > 50\,000$ g mol^{-1} as seen in Fig. 11 where data for P108 and P420 lead to $X_{c,threshold}$ of 5 and *ca* 1%, respectively. $X_{c,threshold}$ is plotted *versus* molecular weight in a double logarithmic plot in Fig. 12. For M_w greater than *ca* 100 000 g mol^{-1}, only incipient levels of crystallinity enable a melt topology that allows retention of melt memory at high temperatures. The $X_{c,threshold}$ decreases with M_w as expected because the process to build sufficient entanglements to prevent memory dissolution in a more viscous high molar mass melt is easier.[35] One can also see clearly from this figure that major changes in the topology of the melt associated with melt memory take place for $M_w > 50\,000$ g mol^{-1} for these copolymers. Since lack of or insignificant time dependence of the effect of melt memory was also observed for $M_w > 50\,000$ g mol^{-1}, we conclude that the topological constraints in the melt, especially those that build near the surface of the crystallites and are associated with melt memory, saturate for these copolymers at a molecular weight of *ca* 50 000 g mol^{-1}. The HPBDs studied here have *ca* 2.2 mol% ethyl branches, but it is expected that $X_{c,threshold}$ and the M_w required to observe changes in melt memory with time would be a function of the copolymer branching composition. Furthermore, any possible correlation of the data of Fig. 12 with melt self-diffusion as

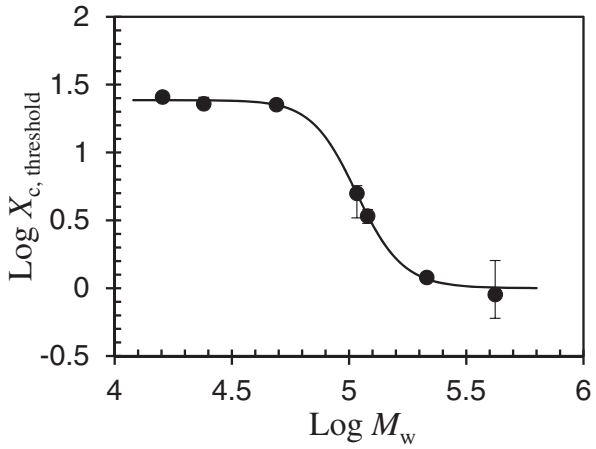

Figure 12. Molecular weight dependence of the threshold crystallinity to observe melt memory from the melt at 140 °C for HPBDs with similar branch content (*ca* 2.2 mol%).

predicted by reptation theory ($D \sim M_w^{-2}$)[48] cannot be established because, as shown in Fig. 12, the log–log plot is not linear.

Temperature dependence of threshold level of crystallinity for melt memory

Data of $X_{c,threshold}$ at different T_{melt} were obtained for P108 ($M_w = 108\,000$ g mol^{-1}) and P195 ($M_w = 214\,500$ g mol^{-1}) at heterogeneous T_{melt} of 130, 140, 150 and 155 °C using the experimental protocol described earlier. The data for P108 are shown in Fig. 13(a) where $\Delta T_{c,peak}$ is plotted instead of $T_{c,peak}$ *versus* the initial crystallinity level. Here, $\Delta T_{c,peak}$ is taken as the difference between $T_{c,peak}$ obtained by cooling from a heterogeneous T_{melt} that was approached with a certain X_c, and the $T_{c,peak}$ obtained from the same T_{melt} approached from above ($X_c = 0$). Thus, all memory is dissolved when $\Delta T_{c,peak} = 0$. As mentioned earlier, $X_{c,threshold}$ is a measure of topological requirements for incipient melt memory, and is determined at the upturn point where $\Delta T_{c,peak}$ departs from zero, as indicated by the dashed lines in the figure. For each T_{melt} tested, $\Delta T_{c,peak}$ deviates from zero at values of X_c that increase with T_{melt}. The increase of $X_{c,threshold}$ with T_{melt} follows the expected higher levels of crystallinity required with increasing T_{melt} for the manifestation of melt memory as segmental transport increases at the higher temperatures. Hence, a higher content of the constraints that build with increasing crystallinity is needed to retain memory in these copolymers when T_{melt} increases.

$X_{c,threshold}$ is a temperature-dependent parameter characteristic of the process of melt memory that follows Arrhenius behavior independently of molecular weight (Fig. 13(b)). A linear correlation is found for both samples with basically the same slope, indicating that the process leading to melt memory is thermally activated with activation energy of 108 ± 6 kJ mol^{-1} independent of molecular weight. Compared with the activation energies given for melt self-diffusion (*ca* 26 kJ mol^{-1}),[40] and the melt flow activation energy from zero-shear viscosity measurements (*ca* 30 kJ mol^{-1}) for the same copolymers,[39] the value to enable melt memory by increasing crystallinity is over three times higher, again indicating that melt memory is a more energy-demanding process. Evidence of a thermally activated process was found recently for polyisoprenes that display identical diffusional activation energy for samples with different molecular weight.[49]

Finally, we offer some interpretation of the almost 1 order magnitude difference between the activation energy obtained from the $X_{c,threshold}$ measurements (108 kJ mol^{-1}) and that from time–temperature superposition analysis of the time-dependent data carried out in the first part of this work (1100 kJ mol^{-1}). Here, we recall that retardation of dissolution of clusters with increasing temperature was associated with the various stabilities of clusters. The more stable ones, associated with the longest crystalline sequences, survive higher temperatures and longer times resulting in very long characteristic times for dissolution of melt memory. Conversely, $X_{c,threshold}$ measures the amount of crystals required for building sufficient constraints to retain clusters in the melt (or limiting X_c value for incipient memory). In the latter, clusters associated with $X_{c,threshold}$ feature the least stability and are on the edge of 'dying away' within the first 5 min in the melt. However, the time-dependent experiments probe clusters with much higher stability since they withstand the first 5 min and manifest their dissolution process within the rest of the 20 h. Although the framework of transporting ethylene sequences is the same, the crystallinity effect and time-dependent experiments sample two different features. The former explores the process to enable melt memory which has lower activation energy than the limiting step for dissolution of melt memory in the latter for which the estimated activation energy is much higher.

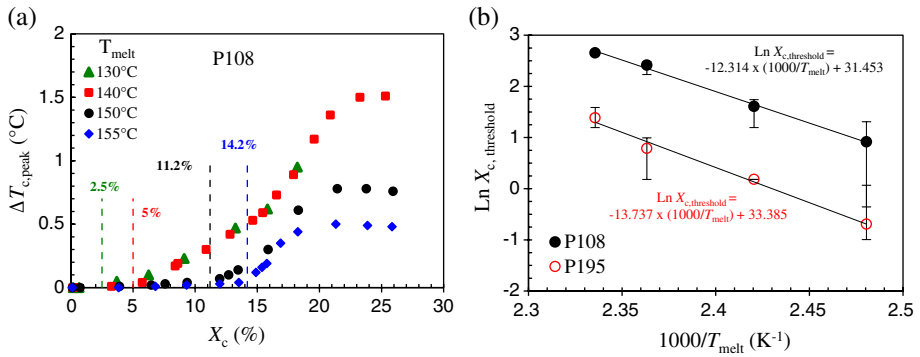

Figure 13. (a) Plot of $\Delta T_{c,peak}$ against degree of crystallinity (X_c) achieved by partial crystallization prior to approaching T_{melt} for P108. (b) Arrhenius-type temperature dependence of $X_{c,threshold}$ for HPBDs (P108 and P195) with similar branch content (*ca* 2.2 mol%) and different molecular weight (108 000 and 214 500 g mol^{-1}).

CONCLUSIONS

Melt annealing time dependence of the strong melt memory effect above the equilibrium melting temperature in model random HPBDs has been studied using DSC. Clusters in the melt that contribute to accelerating crystallization partially dissolve upon prolonged annealing. Dissolution of memory with time is readily observed in low-molecular-weight HPBD (16 000 g mol^{-1}) and is beyond experimental resolution in HPBDs with molecular weight greater than 50 000 g mol^{-1} due to slow segmental diffusion. Dissolution of clusters of high-molecular-weight copolymers is greatly enhanced by the addition of a low-molecular-weight component, exemplifying the role of the low-molecular-weight chains in dissolution of memory. The characteristic times associated with the exponential process of dissolution of memory (hundreds of minutes) are several orders of magnitude larger than the single-chain relaxation time (1 ms–10 s) suggesting that melts with crystallization memory are complex metastable states requiring much higher energy to dissolve clusters than to diffuse the single chain. The increasing characteristic times with melt temperature are associated with a higher stability of the remaining clusters. This is a feature further supported by time–temperature superposition of crystallization data associated with dissolution of memory. The apparent activation energy extracted from these data, 1100 kJ mol^{-1}, is very similar to values reported to dissolve shish structures that form in flow-induced high-density polyethylene.

The effects of molecular weight and melt temperature on the threshold crystallinity level for observing melt memory ($X_{c,threshold}$) were also studied for HPBDs in a range of molecular weights from 16 000 to 420 000 g mol^{-1}. $X_{c,threshold}$ decreases with increasing molecular weight due to slower sequence diffusion in the more viscous melt of high-molar-mass chains. Analogous to the very slow time dependence for dissolution of melt memory, $X_{c,threshold}$ decreases sharply for $M_w > 50\,000$ g mol^{-1}. $X_{c,threshold}$ follows an Arrhenius temperature dependence with activation energy independent of molecular weight, thus indicating that the process leading to melt memory is thermally activated. The activation energy estimated from the temperature dependence of $X_{c,threshold}$ (*ca* 108 kJ mol^{-1}) is about four times the diffusional activation energy of HPBD (*ca* 26 kJ mol^{-1}) and about three times the flow activation energy (*ca* 30 kJ mol^{-1}), indicating that the process of dissipating clusters of ethylene sequences in the melt requires high energy.

ACKNOWLEDGEMENTS

This paper is dedicated to Dr. Vincent BF Mathot on the occasion of his retirement. Funding by the National Science Foundation, Polymer Program DMR 1607786, is gratefully acknowledged.

REFERENCES

1 Fillon B, Wittmann JC, Lotz B and Thierry A, *J Polym Sci B: Polym Phys* **31**:1383–1393 (1993).
2 Michell RM, Mugica A, Zubitur M and Muller AJ, *Adv Polym Sci* **276**:215–256 (2016).
3 Xu J, Ma Y, Hu W, Rehahn M and Reiter G, *Nat Mater* **8**:348–353 (2009).
4 Wunderlich B, *Macromolecular Physics*. Academic Press, New York (1976).
5 Mamun A, Umemoto S, Okui N and Ishihara N, *Macromolecules* **40**:6296–6303 (2007).
6 Lorenzo AT, Arnal ML, Sanchez JJ and Muller AJ, *J Polym Sci B: Polym Phys* **44**:1738–1750 (2006).
7 Sangroniz L, Cavallo D, Santamaria A, Muller AJ and Alamo RG, *Macromolecules* **50**:642–651 (2017).
8 Sangroniz L, Barbieri F, Cavallo D, Santamaria A, Alamo RG and Muller AJ, *Eur Polym J* **99**:495–503 (2018).
9 Funaki C, Yamamoto S, Hoshina H, Ozaki Y and Sato H, *Polymer* **137**:245–254 (2018).
10 Reid BO, Vadlamudi M, Mamun A, Janani H, Gao H, Hu W *et al.*, *Macromolecules* **46**:6485–6497 (2013).
11 Mamun A, Chen X and Alamo RG, *Macromolecules* **47**:7958–7970 (2014).
12 Gao H, Vadlamudi M, Alamo RG and Hu W, *Macromolecules* **46**:6498–6506 (2013).
13 Wang Y, Lu Y, Zhao J, Jiang Z and Men Y, *Macromolecules* **47**:8653–8662 (2014).
14 Fernandez-dArlas B, Balko J, Baumann RP, Poselt E, Dabbous R, Eling B *et al.*, *Macromolecules* **49**:7952–7964 (2016).
15 Luo C and Sommer JU, *Phys Rev Lett* **112**:195702 (2014).
16 Luo C and Sommer JU, *Macro Lett* **5**:30–34 (2016).
17 Alfonso GC and Ziabicki A, *Colloid Polym Sci* **273**:317–323 (1995).
18 Supaphol P and Lin JS, *Polymer* **42**:9617–9626 (2001).
19 Supaphol P and Spruiell JE, *J Appl Polym Sci* **75**:337–346 (2000).
20 Cho K, Saheb DN, Choi J and Yang H, *Polymer* **43**:1407–1416 (2002).
21 Androsch R and Wunderlich B, *Macromolecules* **33**:9076–9089 (2000).
22 Hafele A, Heck B, Hippler T, Kawai T, Kohn P and Strobl G, *Eur Phys J E* **16**:217–224 (2005).
23 Maus A, Hempel E, Thurn-Albrecht T and Saalwaechter K, *Eur Phys J E* **23**:91–101 (2007).
24 Thomas D and Cebe P, *J Therm Anal Calorim* **127**:885–894 (2017).
25 Ergoz E, Fatou JG and Mandelkern L, *Macromolecules* **5**:147–157 (1972).
26 De Rosa C, Auriemma F, Vinti V and Galimberti M, *Macromolecules* **31**:6206–6210 (1998).
27 Hu W, Mathot VBF, Alamo RG, Gao H and Chen X, *Adv Polym Sci* **276**:1–43 (2016).
28 Guan X, Gao H, Zha L, Wu Y and Hu W, *Polymer* **98**:282–286 (2016).
29 Chen X, Mamun A and Alamo RG, *Macromol Chem Phys* **216**:1220–1226 (2015).
30 Hamad FG, Colby RH and Milner ST, *Macromolecules* **48**:7286–7299 (2015).
31 Muthukumar M, *J Chem Phys* **145**:031105 (2016).
32 Schamme B, Dargent E and Fernandez-Ballester L, *Macromolecules* **50**:6396–6403 (2017).
33 Hashimoto M, O'ishi J, Moriya S and Fujiwara S, *Polym J* **47**:481–486 (2015).
34 Flory PJ, *Trans Faraday Soc* **51**:848–857 (1955).
35 Berry GC and Fox TG, *Adv Polym Sci* **5**:261–357 (1968).
36 Zhao J, Sun Y and Men Y, *Ind Eng Chem Res* **56**:198–205 (2017).
37 Li W, Wu X, Chen X and Fan Z, *Eur Polym J* **89**:241–248 (2017).
38 Ziabicki A and Alfonso GC, *Colloid Polym Sci* **272**:1027–1042 (1994).
39 Tao H, Lodge TP and Meerwall EDV, *Macromolecules* **33**:1747–1758 (2000).
40 Bartels CR, Crist B and Graessley WW, *Macromolecules* **17**:2702–2708 (1984).
41 Klein J and Briscoe BJ, *Proc R Soc Lond A* **365**:53–73 (1979).
42 Schuman T, Stepanov EV, Nazarenko S, Capaccio G, Hiltner A and Baer E, *Macromolecules* **31**:4551–4561 (1998).
43 Graessley WW, *Adv Polym Sci* **47**:67–117 (1982).
44 Ecksterin A, Suhm J, Friedrich C, Maier RD, Sassmannshausen J, Bochmann M *et al.*, *Macromolecules* **31**:1335–1340 (1998).
45 Ma Z, Balzano L and Peters GWM, *Macromolecules* **49**:2724–2730 (2016).
46 Alamo R, Domszy RC and Mandelkern L, *J Phys Chem* **88**:6587–6595 (1984).
47 Mandelkern L and Alamo RG, *Physical Properties of Polymers Handbook*, 2nd edn. Springer, New York (2007).
48 De Gennes PG, *J Chem Phys* **55**:572–579 (1971).
49 Wang M, Timachova K and Olsen BD, *Macromolecules* **48**:3121–3129 (2015).

